No cryosphere-confined aquifer below InSight on Mars

Michael Manga[1], Vanshan Wright[2]

1. Department of Earth and Planetary Science, University of California, Berkeley, CA, 94720-4767, USA
2. Geology and Geophysics Department, Woods Hole Oceanographic Institution, MA, 02543-1050, USA

Abstract

The seismometer deployed by the InSight lander measured the seismic velocity of the Martian crust. We use a rock physics model to interpret those velocities and constrain hydrogeological properties. The seismic velocity of the upper ~10 km is too low to be ice-saturated. Hence there is no cryosphere that confines deeper aquifers. An increase in seismic velocity at depths of ~10 km could be explained by a few volume percent of mineral cement (1-5%) in the pores and may document the past or present depth of aquifers.

Plain Language Summary

Large amounts of water may be stored in the Martian crust and episodically released to flood the surface. Where this water exists, and even why, is uncertain. The seismometer on the InSight lander measured the speed of seismic waves in the Martian crust. The presence of ice and water affects seismic velocity. We argue that the measurements preclude a layer of ice-filled crust that confines liquid water in an aquifer.

Key points

- We interpret the seismic wave velocity of the Martian crust measured by InSight.
- We quantity the effects of ice and water on seismic velocity using a rock physics model.
- Measurements preclude a layer of ice-filled upper crust that confines liquid water in an aquifer.

1. Introduction

Large volumes of water are hypothesized to have carved and passed through the Martian outflow channels (e.g., Baker, 2001). Because these channels originate from discrete sources, a groundwater origin is typically invoked (e.g., Head et al., 2003). Given the large discharges needed to create the observed landforms, in some cases a couple orders of magnitude greater than the largest catastrophic floods on Earth (Baker, 1982), large and permeable aquifers would be needed (e.g., Carr, 1979; Manga 2004). While most of the outflow channels are Hesperian (e.g., Tanaka, 1997), their formation continued through the Amazonian (e.g., Rodriguez et al., 2015). Some of the youngest channels originated from fissures in Eastern Elysium Planitia within the past 10s of millions of years (Burr et al., 2002; Voight and Hamilton, 2017). The subsurface of Mars thus appears to have hosted and episodically released large volumes of water over most of Martian history. Hence, detecting the presence and quantifying the volume of subsurface water and ice would help constrain the water budget and cycle from the Noachian to present (Clifford and Parker, 2001).

To discharge water at the surface, aquifers must have sufficient pressure for water to reach the surface. One way to achieve hydraulic heads greater than hydrostatic and hence enable surface discharge is to confine aquifers beneath an overlying ice-saturated crust or cryosphere (e.g., Carr, 1996; Harrison and Grimm, 2004; Andrews-Hanna and Phillips, 2007). As Mars cools and this cryosphere thickens, hydraulic heads will increase and may also create the pressure needed to fracture the crust (Wang et al., 2006). The MARSIS and SHARAD radar systems on Mars have not detected such aquifers. Other geophysical data, such as shear wave velocity, Vs, may be useful because Vs is sensitive to physical properties of the subsurface.

Our objective is to interpret Vs measured by the InSight mission in Elysium Planitia. We use rock physics models to compute effective medium properties and to help distinguish between porous basalt filled with gas, liquid water, ice, or mineral cement. We focus on two observations. First, Vs within Mars' upper ~8-11 km is ~1.7-2.1 km/s (Longnonné et al., 2020) and possibly lower (Knapmeyer-Endrun et al., 2020). Longnonné et al. (2020) attribute these relatively low Vs to "highly altered and or damaged layers." Second, receiver function analyses suggest that Vs increases by ~0.4-1 km/s below depths of ~8-11 km (Figure S4-9c in Longnonné et al., 2020).

2. Model

We constrain Mars' subsurface hydrology by comparing Vs computed from InSight seismometer data with Vs modeled for gas, liquid water, and ice-filled porous basalt. We estimate Vs from the effective elastic moduli (bulk and shear moduli) and bulk density of basalt. In the absence of information on the nature of the actual pore space, we model the pore space with randomly-oriented oblate ellipsoidal inclusions with specified aspect ratios. We compute effective elastic moduli with a so-called self-consistent approximation based on the elastic deformation of single inclusion embedded in a background medium with the elastic properties of the effective medium. For gas and ice-saturated pores, for the shear modulus μ and bulk modulus K, we use the Wu (1966) self-consistent (subscript SC) moduli estimates

$$\mu_{SC}^{*} = \mu_m + \phi(\mu_i - \mu_m)Q^{*} \quad (1)$$

and

$$K_{SC}^{*} = K_m + \phi(K_i - K_m)P^{*} \quad (2)$$

where i and m represent inclusion and matrix values, * represents effective medium values, ϕ is the volume fraction of inclusions, and Q and P are geometric shape factors for the inclusion that depend on μ_{SC}^{*} and K_{SC}^{*} (Berryman, 1980). Aspect ratio is the minor axis divided by the major axis; more elongate pores have smaller aspect ratios. Equations (1-2) are coupled and hence are solved by simultaneous iteration. Bulk density is based on the volume-weighted average,

$$\rho^{*} = (1-\phi)\rho_m + \phi\rho_i. \quad (3)$$

Vs is then computed by

$$\mathrm{Vs} = \sqrt{\frac{\mu_{SC}^{*}}{\rho^{*}}}. \quad (4)$$

We estimate Vs for water-filled pores by using Gassmann-Biot theory to saturate dry inclusions (page 169 of Mavko et al., 1998). This is appropriate for frequencies < 100 Hz, and hence the frequency of seismic waves on Mars, where there is no relative motion between fluids and solids and thus no frequency-dependence of Vs.

We use elastic moduli and bulk densities for basalt compiled in Heap (2019), summarized in table 1. We choose basalt for the solid phase because it should dominate the subsurface beneath InSight

(Golombek et al., 2020). Vacuum versus gas-filled pores will have negligible effects on results and conclusions because gas density is significantly lower than basalt and liquid water densities, and gas compressibility is significantly greater than the compressibility of basalt and liquid water.

Table 1: Properties of materials in the Martian crust that affect seismic velocity (from Heap, 2019).

	Density (kg/m^3)	Bulk modulus K (Pa)	Shear modulus μ (Pa)
Basalt solids	2900	8.0×10^{10}	4.0×10^{10}
Liquid water	1000	2.2×10^{9}	0
Water ice	910	8.1×10^{9}	3.7×10^{9}
Gas	1.8	1.0×10^{5}	0

3. Results

We consider porosities ($= 100 \times \phi$) up to 30% and pore aspect ratios from 0.03 to 1. For ice-saturated basalt, Vs is always intermediate between that of ice and solid basalt, and Vs is always greater than 2.6 km/s (Figure 1). Increasing porosity and pore oblateness both decrease velocity. Replacing the ice with gas lowers Vs by lowering shear modulus more than bulk density (Figure 2). Because water and gas shear moduli are zero, and water is denser than gas, replacing gas with water decreases Vs. In passing from a gas- to water-saturated crust, we should thus expect Vs to decrease a small amount, assuming that the pores do not change (Figure 3).

4. Discussion

Uncertainties in measured Vs and approximations inherent in the model guide our interpretations. There are uncertainties in the magnitude of Vs, the depth of changes, and the sharpness of Vs-depth change (Lognonné et al., 2020). The rock physics model is idealized, though it can reproduce measured Vs-porosity relationships in Earth basalts (e.g., Heap, 2019). Natural sedimentary and igneous rocks beneath the InSight lander likely contain multiple pore structures ranging from fractures to intergranular pores in sediments and vesicles in volcanic rocks. In the absence of detailed information about subsurface lithology and velocity-depth profiles (e.g., borehole vertical seismic profiling velocities), we represent the subsurface with a homogeneous, isotropic porous material. With these limitations in mind, we focus on the most robust inferences that should not be sensitive to uncertain details in the observations and idealizations in the model.

4.1 No thick, ice-saturated cryosphere

Vs of 1.7-2.1 km/s in the upper 8-11 km of the crust beneath Insight (Longnonné et al., 2020) is similar to or lower than standard pure ice Vs (2.0 km/s) (Gagnon et al., 1988). No rock physics modeling is thus needed to conclude that the low measured velocities are incompatible with an ice-saturated regolith or crust. Predicted ice-filled Vs (Figure 1) is also much larger than observed Vs, even for high porosity (30 %) and very elongated (aspect ratio = 0.03) pores.

4.2 Evidence for an aquifer

Replacing ice with gas or liquid water in the pores of the upper crust greatly reduces Vs to values that can be lower than 2 km/s (Figure 2). For plausible combinations of pore geometries and porosities, with porosities from 5-15% and aspect ratios 0.03 to 0.1, it is possible to obtain the observed upper crustal Vs. For example, Adam and Otheim (2013) used similar rock physics models for Snake River Plain basalt (a reasonable Mars analog) and found that aspect ratios of ~0.02 to 0.1 fit measured velocities and were similar to pores imaged directly in computed tomography models. A porosity of 10%, for example, implies a dry density of 2610 kg/m^3 (and water-saturated density of 2710 kg/m^3), similar to some estimates of the bulk crust density of 2582$\pm$209 kg/m^3 (Goossens et al., 2017). Thus, based on measured velocities, analogue materials, and estimated densities, a gas or liquid filled crust is most consistent with the InSight measurements. Patchy ice saturation may also be possible – adding some ice will lead to velocities intermediate between those shown for dry and ice-saturated materials (Figure 2 and 3).

It is challenging to distinguish between water and gas-filled pores. Since the shear modulus is the same for both fluids, and the bulk density increase from saturating pores with water is small, there is only a relatively small decrease in Vs when transitioning from dry to water-saturated rocks (Figure 3). For properties that lead to Vs <2 km/s, the change in velocity is usually less than 100 m/s. Velocity reductions <100 m/s are smaller than the uncertainties in velocities and velocity changes. A velocity decrease that might demark the top of an aquifer has not yet been identified or inferred within the crust.

Vs may increase by 0.5 to 1 km/s at depths between 8 and 11 km owing to decreases in porosity and/or increases in pore aspect ratio, assuming no lithology changes. For illustrative purposes, consider a porosity of 10%, for which an (reasonable) aspect ratio of 0.06 (Adam and Otheim, 2013) leads to a velocity of ~2 km/s for dry or wet rocks, and similar to the Martian upper crust. Slightly less elongated pores (aspect ratio 0.08) will raise the velocity by ~0.5 km/s. Alternatively, decreasing porosity by ~2 % would cause the same increase in velocity. Two possible ways of decreasing porosity and/or increasing pore aspect ratios are via cementation and compaction.

Cementation can decrease pore elongation and porosity simultaneously via precipitation of minerals at narrow pore apertures. Sequestering 1 bar of CO_2 as carbonate cement requires 1 weight % cement over a depth range of 2 km (e.g., Kite and Daswani, 2019). Assuming a heat flow of ~18 mW/m^2 (Parro et al., 2017), a thermal conductivity of 2-3 W/mK (Gyalay et al., 2020), and a mean surface temperature of 70 K below freezing, the melting temperature of ice is reached at a depth of 7.8-11.7 km – with considerable depth uncertainty owing to uncertainty in the heat flow and thermal conductivity. The depth of the velocity increase is similar to the depth at which liquid water would be stable at present and in the past. Depending on the pore geometry and porosity, between about 1 and 5 volume % precipitated carbonates may explain the observed increase in Vs, assuming similar mineral properties for basalt and carbonate cement.

Viscous creep-induced compaction and pore closure can also decrease porosity and increase aspect ratio (less elongated pores) and has been suggested as the cause of the velocity increase (Gyalay et al., 2020). Since compaction has an exponential time dependence and viscosity depends exponentially on temperature, the porosity change has a double exponential dependence on temperature leading to a very sharp and near-complete porosity reduction below some depth. If this were the case, we should expect Vs to increase to ~3.7 km/s (larger than observed) unless subsequent processes such as impacts, tectonics, and thermal stresses created new porosity and fractures.

In the present study, we focus on Vs as a probe of subsurface hydrogeology. InSight offers other opportunities to search for confined aquifers. If fluid pressure in a cryosphere or otherwise confined aquifer is high, the state of stress may be close to that needed to initiate slip on faults, and tidal stresses may trigger marsquakes (Manga et al., 2019; Heimisson and Avouac, 2020). Unfortunately, the large diurnal variations in noise, and hence the ability to detect marsquakes (Giardini et al., 2020), makes it somewhere between very difficult and impossible to identify any tidal modulation of seismicity.

5. Conclusions

The uncertainties in Vs-depth profiles provide some limitations on quantifying Mars' subsurface hydrogeology. Assuming that Vs is ~2 km/s or lower in the upper ~8-10 km of the crust and there are sharp or gradual Vs increases of ~0.5-1 km/s at greater depths does, however, allow us to draw some general conclusions. These units are unlikely to be ice-saturated. Hence there cannot be a confining cryosphere above any groundwater unless the layer is thin enough to be (currently) seismically undetectable. Whether or not *unconfined* liquid water aquifers exist cannot be robustly constrained by the published Vs models because the presence of water versus gas has a small effect on Vs. However, the velocity increase at a depth of 8-11 km could be explained by the presence of a few volume percent of mineral cement such as carbonates precipitated from groundwater, which may be indirect evidence for large volumes of past or current groundwater.

Acknowledgments: The authors thank the InSight team for their dedication and remarkable accomplishments. MM was supported by NASA grant 80NSSC19K0545.

References cited

Adam, L., & Otheim, T. (2013). Elastic laboratory measurements and modeling of saturated basalts. *Journal of Geophysical Research: Solid Earth*, *118*(3), 840-851.

Andrews-Hanna, J. C., & Phillips, R. J. (2007). Hydrological modeling of outflow channels and chaos regions on Mars. *Journal of Geophysical Research: Planets*, *112*(E8).

Baker, V. R. (1982). The channels of Mars. *Bristol: Hilger*.

Baker, V. R. (2001). Water and the Martian landscape. *Nature*, *412*(6843), 228-236.

Berryman, J. G. (1980). Long-wavelength propagation in composite elastic media II. Ellipsoidal inclusions. *The Journal of the Acoustical Society of America*, *68*(6), 1820-1831.

Burr, D. M., McEwen, A. S., & H. Sakimoto, S. E. (2002). Recent aqueous floods from the Cerberus Fossae, Mars. *Geophysical Research Letters*, *29*(1), 13-1.

Carr, M. H. (1979). Formation of Martian flood features by release of water from confined aquifers. *Journal of Geophysical Research: Solid Earth*, *84*(B6), 2995-3007.

Carr, M. H., & Carr, M. H. (1996). *Water on Mars*. New York: Oxford University Press.

Clifford, S. M., & Parker, T. J. (2001). The evolution of the Martian hydrosphere: Implications for the fate of a primordial ocean and the current state of the northern plains. *Icarus*, *154*(1), 40-79.

Gagnon, R. E., Kiefte, H., Clouter, M. J., & Whalley, E. (1988). Pressure dependence of the elastic constants of ice Ih to 2.8 kbar by Brillouin spectroscopy. *The Journal of chemical physics*, *89*(8), 4522-4528.

Giardini, D., Lognonné, P., Banerdt, W. B., Pike, W. T., Christensen, U., Ceylan, S., ... & Yana, C. (2020). The seismicity of Mars. *Nature Geoscience*, *13*(3), 205-212.

Golombek, M., Warner, N. H., Grant, J. A., Hauber, E., Ansan, V., Weitz, C. M., ... & Banerdt, W. B. (2020). Geology of the InSight landing site on Mars. *Nature communications*, *11*(1), 1-11.

Goossens, S., Sabaka, T. J., Genova, A., Mazarico, E., Nicholas, J. B., & Neumann, G. A. (2017). Evidence for a low bulk crustal density for Mars from gravity and topography. *Geophysical research letters*, *44*(15), 7686-7694.

Gyalay, S., Nimmo, F., Plesa, A. C., & Wieczorek, M. (2020). Constraints on Thermal History of Mars From Depth of Pore Closure Below InSight. *Geophysical Research Letters*, *47*(16), e2020GL088653.

Harrison, K. P., & Grimm, R. E. (2004). Tharsis recharge: A source of groundwater for Martian outflow channels. *Geophysical Research Letters*, *31*(14).

Head, J. W., Wilson, L., & Mitchell, K. L. (2003). Generation of recent massive water floods at Cerberus Fossae, Mars by dike emplacement, cryospheric cracking, and confined aquifer groundwater release. *Geophysical research letters*, *30*(11).

Heap, M. J. (2019). P-and S-wave velocity of dry, water-saturated, and frozen basalt: Implications for the interpretation of Martian seismic data. *Icarus*, *330*, 11-15.

Heimisson, E. R., & Avouac, J. P. (2020). Analytical prediction of seismicity rate due to tides and other oscillating stresses. *Geophysical Research Letters*, *47*(23), e2020GL090827.

Kite, E. S., & Daswani, M. M. (2019). Geochemistry constrains global hydrology on Early Mars. *Earth and Planetary Science Letters*, *524*, 115718.

Knapmeyer-Endrun, B. et al. (2020) New seismological constraints on the crustal structure of Mars and the Moon, AGU asbtract DI026-01.

Lognonné, P., Banerdt, W. B., Pike, W. T., Giardini, D., Christensen, U., Garcia, R. F., ... & Zweifel, P. (2020). Constraints on the shallow elastic and anelastic structure of Mars from InSight seismic data. *Nature Geoscience*, *13*(3), 213-220.

Manga, M. (2004). Martian floods at Cerberus Fossae can be produced by groundwater discharge. *Geophysical Research Letters*, *31*(2).

Manga, M., Zhai, G., & Wang, C. Y. (2019). Squeezing marsquakes out of groundwater. *Geophysical Research Letters*, *46*(12), 6333-6340.

Mavko, G., Mukerji, T., & Dvorkin, J. (1998). *The rock physics handbook*. Cambridge university press.

Parro, L. M., Jiménez-Díaz, A., Mansilla, F., & Ruiz, J. (2017). Present-day heat flow model of Mars. *Scientific reports*, *7*(1), 1-9.

Rodriguez, J. A. P., Kargel, J. S., Baker, V. R., Gulick, V. C., Berman, D. C., Fairén, A. G., ... & Glines, N. (2015). Martian outflow channels: How did their source aquifers form and why did they drain so rapidly?. *Scientific reports*, *5*(1), 1-10.

Tanaka, K. L. (1997). Sedimentary history and mass flow structures of Chryse and Acidalia Planitiae, Mars. *Journal of Geophysical Research: Planets*, *102*(E2), 4131-4149.

Voigt, J. R., & Hamilton, C. W. (2018). Investigating the volcanic versus aqueous origin of the surficial deposits in Eastern Elysium Planitia, Mars. *Icarus*, *309*, 389-410.

Wang, C. Y., Manga, M., & Hanna, J. C. (2006). Can freezing cause floods on Mars?. *Geophysical research letters*, *33*(20).

Wu, T. (1966). The effect of inclusion shape on the elastic moduli of a two-phase material. *International Journal of solids and structures*, *2*(1), 1-8.

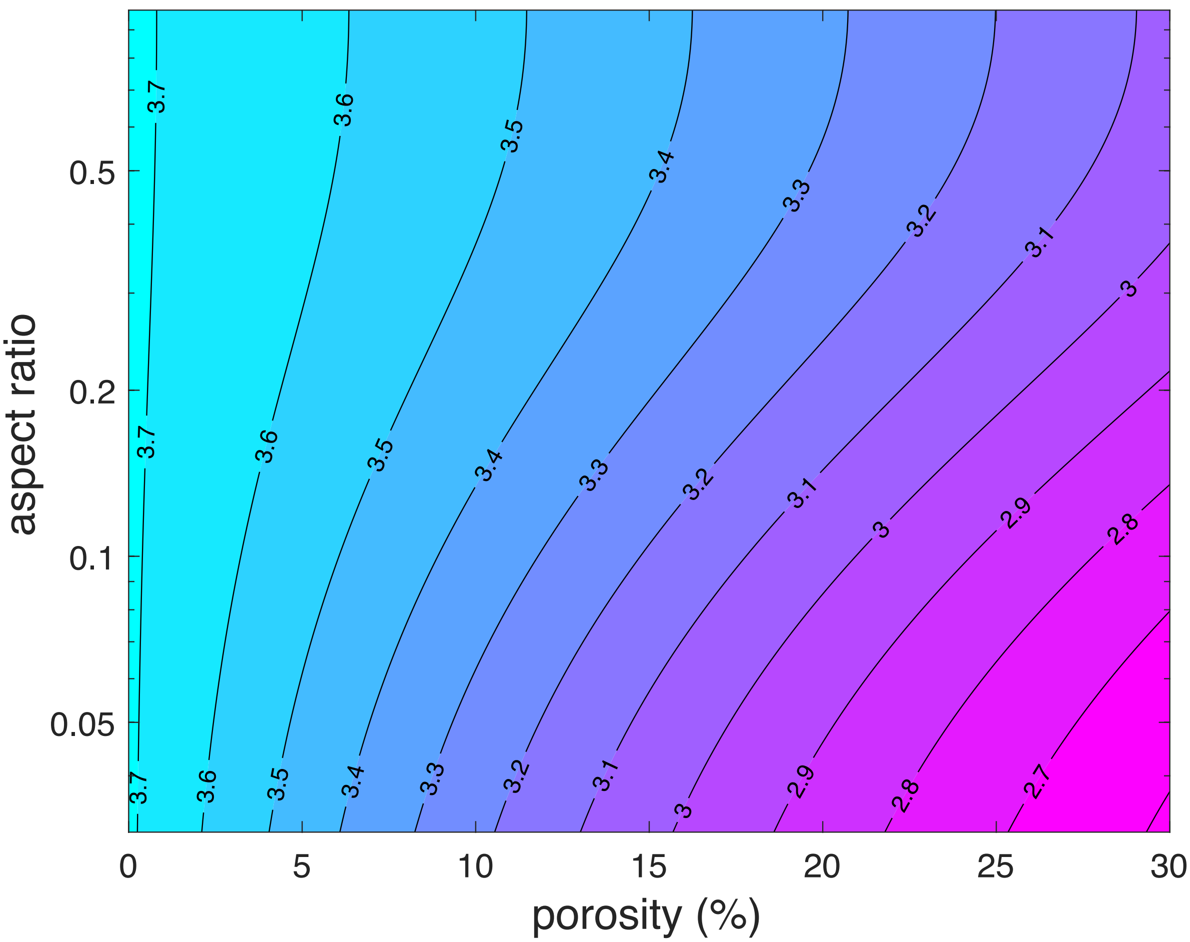

Figure 1: Vs (contours in km/s) for ice-filled ellipsoidal pores as a function of aspect ratio and porosity. All these velocities exceed that of the upper 8-11 km of the Martian crust.

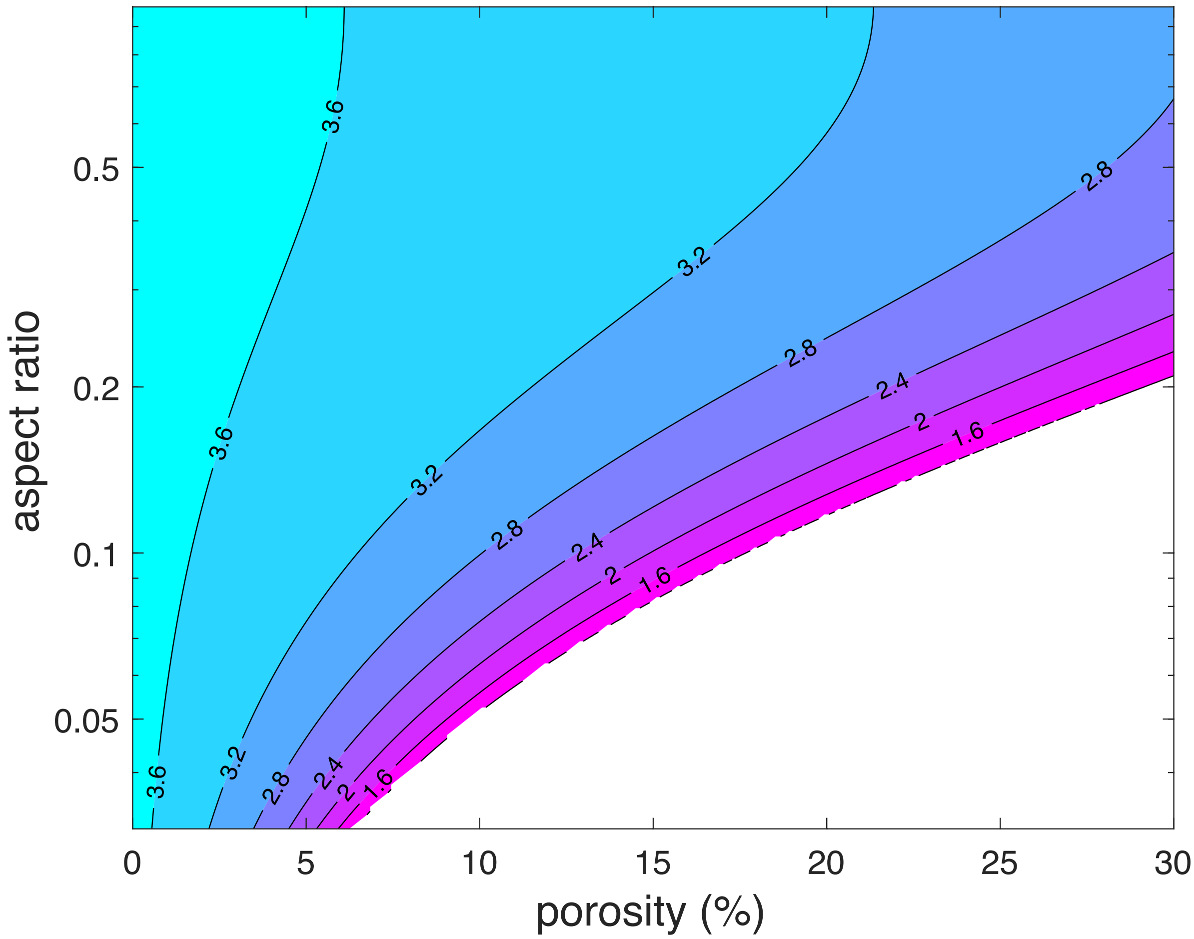

Figure 2: Vs (contours in km/s) for gas-filled ellipsoidal pores as a function of aspect ratio and porosity. White shows regions where the Wu (1966) leads to unphysical velocities as approximations break down.

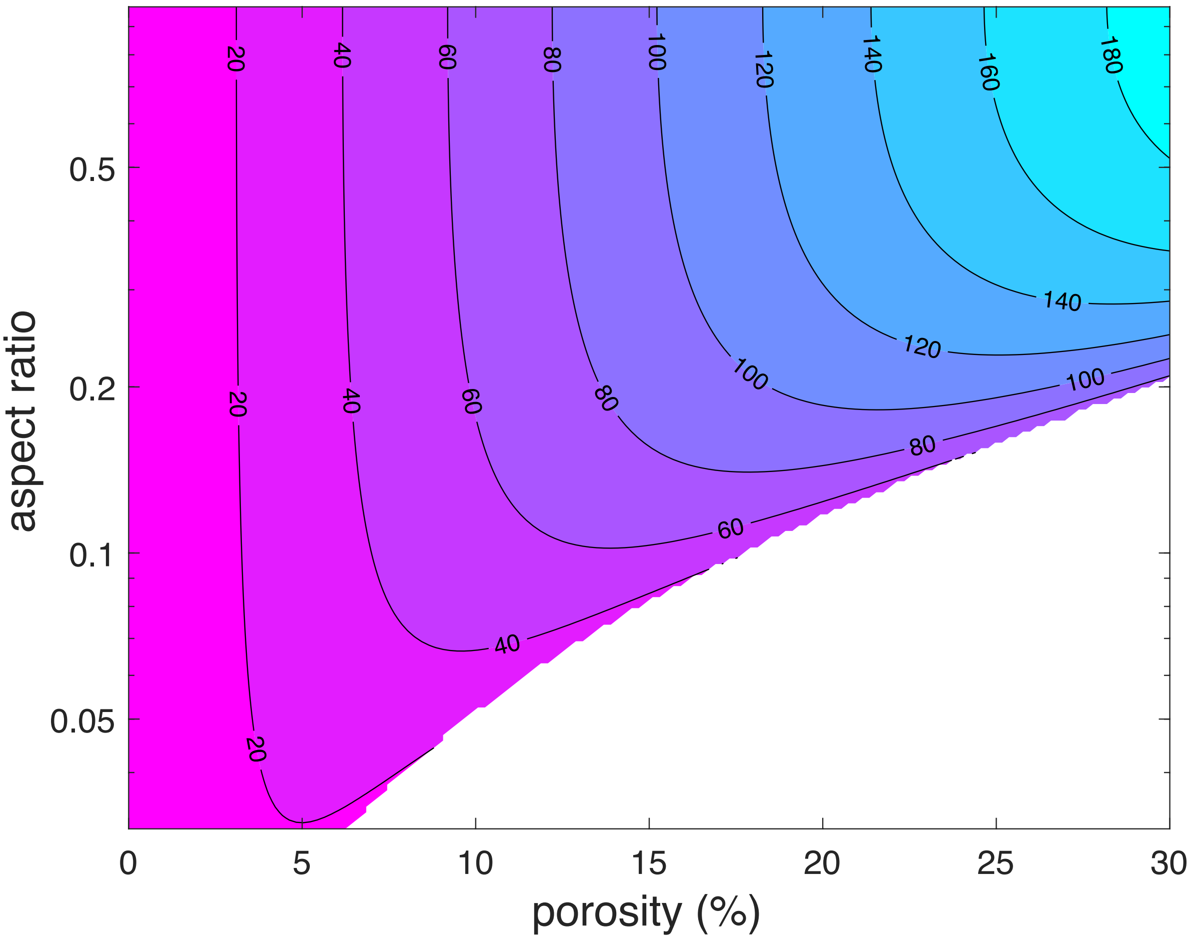

Figure 3: Difference in Vs of gas-filled and liquid water-filled pores (contours in m/s). Vs should decrease upon entering a water-saturated aquifer. Velocity changes from saturating an aquifer are probably too small to detect unless pore geometry and/or porosity also change. White shows regions where the Wu (1966) leads to unphysical velocities as approximations break down.